processes

Article

A Modified Multiparameter Linear Programming Method for Efficient Power System Reliability Assessment

Jing Zuo, Sui Peng *, Yan Yang, Zuohong Li, Zhengmin Zuo, Hao Yu and Yong Lin

Grid Planning and Research Center, Guangdong Power Grid Corporation, CSG, Guangzhou 510080, China
* Correspondence: pengsui@gd.csg.cn; Tel.: +86-188-2003-8903

Abstract: Power systems face adequacy risks because of the high integration of renewable energy. It is urgent to develop efficient methods for power system operational reliability assessment. Conventional power system reliability assessment methods cannot achieve real-time assessment of system risk because of the high computational complexity and long calculation time. The high computational complexity is mainly caused by a large number of optimal power flow (OPF) calculations. To reduce the computational complexity, this paper transfers the optimal power flow model as a multiparameter linear programming model. Then, the optimal power flow can be obtained by linear calculations. Furthermore, this paper proposes a state reduction method considering the importance index of transmission lines for further improving the calculation efficiency. Case studies are carried out on IEEE standard systems and a provincial power grid in China. Compared with the conventional reliability assessment method, the reliability assessment efficiency of the proposed method increases by 10–40 times, and the assessment error is less than 1%.

Keywords: power system reliability; state reduction; multiparameter linear programming; optimal power flow; computational complexity

check for updates

Citation: Zuo, J.; Peng, S.; Yang, Y.; Li, Z.; Zuo, Z.; Yu, H.; Lin, Y. A Modified Multiparameter Linear Programming Method for Efficient Power System Reliability Assessment. *Processes* **2022**, *10*, 2188. https://doi.org/10.3390/pr10112188

Academic Editor: Masoud Soroush

Received: 28 September 2022
Accepted: 23 October 2022
Published: 25 October 2022

1. Introduction

To cope with environmental and climate challenges, vigorously developing renewable energy such as wind and solar power has become a popular choice for countries around the world in formulating energy policies and promoting clean energy transitions [1,2].

With the high penetration of renewable energy integrating into the power system, the operational risk of the power system is prominent [3]. Risk evaluation becomes more complex, and they include not only the occasional failure of power equipment but also random fluctuations on the supply side and uncertainty on the demand side [4]. These factors easily induce a reliability risk for the power supply and demand mismatch in the power system. Therefore, the real-time evaluation of power system reliability levels is particularly important.

Existing reliability assessment methods are mainly used to carry out reliability assessments in traditional power systems' medium- or long-term planning stage and they cannot meet the time requirements of real-time reliability assessments of power systems [5,6]. In addition, due to the more complex risk incentives of power systems, equipment failure, and other sudden disturbances cannot be accurately described in a medium- or long-term reliability assessment [7]. Therefore, it is urgent to propose a fast reliability assessment algorithm for power systems to determine the system's reliability levels real-time.

To improve the efficiency of the reliability assessment, the problems of high computational complexity and long computing time must be addressed. These problems arise because of the large number of system states required for reliability assessment and the high computational complexity of each system state [8]. Thus, system state reduction and state analysis simplification are the main methods for efficiency improvement.

In terms of reducing the number of system states, some scholars have proposed event truncation [9], event screening [10–12], significance sampling [13–15], event segmentation [16], cross-entropy sampling [17–21], Latin hypercube sampling [22–24], uniform sampling [25,26] and other methods to improve the efficiency of sampling events.

In these methods, the system state is regarded as an entirety and the classic system states are generated based on a set of rules. However, these methods still have difficulty achieving the desired significant reduction in the number of events, and the characteristic of the system state is ignored. Note that the system states studied in the reliability evaluation mainly include generator output state, load demand state, and transmission line state. Generally, the generator unit output state and load demand state can be obtained based on historical data, while the transmission line state has strong randomness. It is the transmission line state that highly increases the number of system state. Nevertheless, to the best of our knowledge, few works have paid attention to the state reduction considering the random transmission line reliability.

In terms of system state analysis, many studies have been conducted to improve reliability evaluation efficiency. Examples include nonparametric decomposition based on dimensionality reduction [27], artificial intelligence [28], neural network [29,30], stochastic network flow models [31], minimum cut sets [32], and Bayesian networks [33]. However, the aforementioned methods still need to accomplish highly nonlinear calculations, which is computationally time-consuming.

This paper proposes a modified multiparameter linear programming (MPLP) method for power system reliability assessment efficiency improvement. It is studied from the two perspectives of system state reduction and system state simplification analysis. For system state reduction, the randomness characteristic of the transmission line is stressed. The significant transmission line state which contributes most to the reliability index is sampled. For state analysis simplification, it should be noted that the optimal power flow calculation is the main reason for the high computational complexity in system state analysis. This paper transfers the optimal power flow model to a modified MPLP model. Under this condition, the optimal power flow solution can be obtained through linear calculations, thus greatly improving the efficiency of system state analysis. Thus, the contradiction between system reliability assessment efficiency and accuracy is solved. Case studies of reliability test systems are carried out on the Roy Billinton test system (RBTS), IEEE-RTS 79, IEEE-RTS 96, and a provincial power grid in China to show the effectiveness of the proposed method.

2. System State Generation Method Considering Transmission Line Importance

This section introduces the transmission line importance-based system state generation method. The importance index of transmission line status is proposed. The influence of different transmission line states on the power flow distribution of the system is calculated and analyzed to select the critical transmission line status that contributes greatly to the reliability index.

2.1. Transmission Line Status Importance Index

This subsection quantifies the influence of the transmission lines on the power flow through the importance index of the transmission lines and generates the statuses of critical transmission lines. If a transmission line fault leads to a great change in the power flow distribution of the system, the line is more important, and it has a larger importance index.

The importance index of transmission lines includes the traditional importance index of transmission lines and the importance index of transmission lines considering the fault probability. Details are described below.

(1) Traditional importance index of transmission lines

The traditional importance index of transmission lines, denoted as I_{tra}, quantifies the relationship between the actual active power flowing on the transmission line and the transmission capacity, which is expressed as

$$I_{tra} = \sum_{i=1}^{N_l} w_i \left(\frac{F_i}{F_i^{max}} \right)^{2m} \tag{1}$$

where F_i is the actual active power flow of line i, ${F_i}^{max}$ is the upper limit of the active power capacity of line i, and w_i is the weighting factor of line i reflecting the relative importance of each line, which can be determined according to engineering experience. N_l is the number of transmission lines in the system, and m is the integer index of I_{tra}.

(2) Importance index of transmission lines considering the fault probability

The fault probability of transmission lines is taken into account, and the influence of the fault probability and active power on the power flow is quantified. Suppose there are N_l transmission lines in the system. The fault probability importance index denoted as I_{pro}, can be expressed as

$$I_{pro} = P_c \cdot \sum_{i=1}^{N_l} w_i \left(\frac{F_i}{F_i^{max}} \right)^{2m} \tag{2}$$

where P_c is the probability of failure of the Nd transmission lines (N_d = 1, 2, . . . , N_l) such that

$$P_c = \prod_{i=1}^{N_d} U_i \cdot \prod_{j=1}^{N_l - N_d} \left(1 - U_j\right) \tag{3}$$

where U_i and U_j are the forced outage rate of the transmission lines with and without failures, respectively.

2.2. Calculation of Transmission Line Status Importance Index

In this subsection, the importance indices of different transmission line states are calculated by given system operation scenarios. The critical transmission line states are selected by summarizing and sorting the importance indices. Furthermore, this paper uses the K-means algorithm to generate representative typical system operation scenarios and calculate their occurrence probability. The K-means algorithm used here is replaceable and other methods can also be used to give system operation scenarios to ensure the rationality of the calculation results of importance indices.

The calculation steps of the transmission line status importance index are as follows:

Step 1: Input the historical annual generator output curve and historical annual load curve. The length of the historical time series of generation and load curves both are a year; namely, there are 8760 points for each curve.

Step 2: Determine the number of clusters as N_L according to the system size. Determine the initial clustering center M_{ij}, where i (I = 1~N_L) represents the cluster after clustering and j represents the clustering curve, which can include the generator output curve, load curve, or generator output-load curve.

Step 3: Calculate the average value of the Euclidean distance between points on the curve and each cluster center for each hour; the formula is as follows:

$$D_{ki} = \left[\sum_{j=1}^{N_c} \left[\left(M_{ij} - G_{kj} \right)^2 \right] \right]^{1/2} \tag{4}$$

where D_{ki} is the Euclidean distance from the kth point to the ith cluster center, G_{kj} is the value of the kth point on curve j, and N_c is the number of curves.

Step 4: Assign each point on the curve to the nearest cluster to regroup them to form a new cluster, and calculate the center M_{ij} of the new cluster, as shown in Formula (5).

$$M_{ij} = \sum_{k=1}^{N_i} L_{ki} / N_i \tag{5}$$

where N_i is the number of points in the ith cluster, and L_{ki} is the value of the kth point in the ith cluster on curve j.

Step 5: Repeat Step 3 and Step 4 until the clustering centers of all clusters remain unchanged between the two iterations, yielding the clustering results of the running scenarios.

Step 6: The probability of obtaining the selected running scenario after clustering can be calculated by the following formula:

$$P_l = N_c / N \tag{6}$$

where P_l is the probability of the lth operating scenario, N_c is the number of points clustered in the lth operating scenario, and N is the total number of points on the curve.

Step 7: The importance index for a given operation scenario is calculated according to (1)–(2). Considering all the operation scenarios selected after clustering, the comprehensive importance index of the system state denoted as R, can be calculated by

$$R = \sum_{l=1}^{N_S} P_l \cdot I_l \tag{7}$$

where I_l is the importance index of operation scenario l (including the traditional importance index of transmission lines and the importance index of transmission lines considering the fault probability), P_l is the probability of operation scenario l, and N_S is the number of system operation scenarios selected after clustering.

Step 8: According to the value of the comprehensive importance index R, the critical transmission line status can be determined with different priorities.

2.3. Generating Critical Transmission Line State Set

Based on the above contents, this section summarizes the steps to generate the critical transmission line state set based on the transmission line state importance index. Details are presented below.

Step 1: Input the generator output curve and load curve.

Step 2: Select the operation scenario of the power system by the clustering algorithm.

Step 3: Enumerate the transmission line statuses in the system for each selected operation scenario.

Step 4: Calculate the importance index of each transmission line status. These indices are calculated by considering all selected operation scenarios.

Step 5: Rank the importance of the transmission lines according to the importance index from high to low.

Step 6: Select the required transmission line statuses according to the importance ranking results to determine the critical transmission line statuses.

Step 7: According to the engineers' own experience, the fault statuses of transmission lines with greater impact can be selected as the critical line statuses.

Step 8: Combine the collections obtained in Steps 6 and 7 to establish the final critical transmission line status set.

The proposed method avoids the enumeration of a large number of system states by generating important system states, reduces the number of system states, and ensures reliability assessment accuracy.

3. System State Analysis Method Based on MPLP

The optimal power flow (OPF) calculation is the most time-consuming part of power system reliability evaluation. OPF is a highly nonlinear optimization problem with exponential complexity [34]. To reduce the computational complexity of system state analysis, the OPF model is rewritten as an MPLP model based on the similarity between the OPF model and the MPLP model. The OPF solution can be obtained through linear calculations under certain conditions.

3.1. Basic Principles of Multiparameter Linear Programming

In general, MPLP problems can be described with

$$\begin{aligned} &\min \boldsymbol{z} = c\boldsymbol{x} \\ &s.t.\ \ \boldsymbol{A}_1\boldsymbol{x} = \boldsymbol{b}_1 + \Delta\boldsymbol{b}_1 = \boldsymbol{b}_1 + \boldsymbol{E}_1\boldsymbol{\theta} \\ &\quad\ \ \boldsymbol{A}_2\boldsymbol{x} \leq \boldsymbol{b}_2 + \Delta\boldsymbol{b}_2 = \boldsymbol{b}_2 + \boldsymbol{E}_2\boldsymbol{\theta} \end{aligned} \tag{8}$$

where $\boldsymbol{z}$ is the objective function, $\boldsymbol{x}$ is the decision variable, and c is a constant coefficient. In the constraint conditions, $\boldsymbol{A}_1$ and $\boldsymbol{A}_2$ are constant coefficient matrices, and $\boldsymbol{\theta}$ is a parameter vector. $\Delta\boldsymbol{b}_1$ and $\Delta\boldsymbol{b}_2$ are the uncertainties of the right part of the linear constraint. They are denoted by $\boldsymbol{E}_1\boldsymbol{\theta}$ and $\boldsymbol{E}_2\boldsymbol{\theta}$.

When the parameter vector $\boldsymbol{\theta}$ changes, the right part of the linear constraint changes, and the optimal value $\boldsymbol{z}^*(\boldsymbol{\theta})$ and the optimal solution $\boldsymbol{x}^*(\boldsymbol{\theta})$ change correspondingly. When $\boldsymbol{\theta}$ changes within a certain range $\hat{\boldsymbol{\theta}} = \boldsymbol{\theta} \pm \Delta\boldsymbol{\theta}$, the change in the optimal solution $\boldsymbol{x}^*(\boldsymbol{\theta})$ has an obvious linear relationship with the change in $\boldsymbol{\theta}$: $\boldsymbol{x}^*(\hat{\boldsymbol{\theta}}) = a\hat{\boldsymbol{\theta}} + b$, where $\boldsymbol{a}$ and $\boldsymbol{b}$ are linear parameters related to $\boldsymbol{\theta}$. In this paper, the range of variation is called the critical region, and the linear relationship within the critical region is called the mapping relation. Figure 1 is a schematic diagram of the critical regions of a two-dimensional parameter vector $\boldsymbol{\theta} = (\boldsymbol{\theta}_x, \boldsymbol{\theta}_y)$.

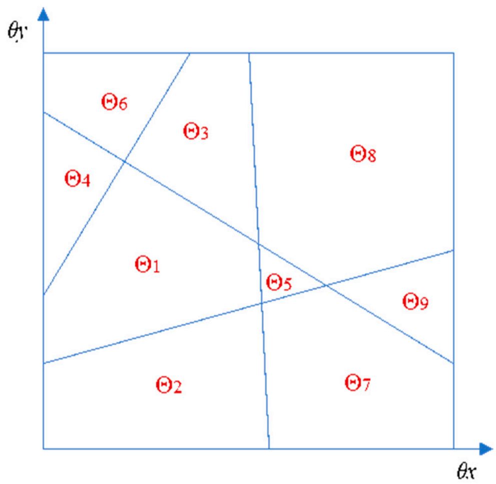

Figure 1. Illustrative diagram of the critical regions in two-dimensional parameter space.

In the MPLP model, for a constraint $f(\boldsymbol{x}) \leq 0$, if the optimal solution $\boldsymbol{x}^*$ satisfies $f(\boldsymbol{x}^*) = 0$, the constraint $f(\boldsymbol{x})$ is called a "strong constraint". Otherwise, it is a "weak constraint". Assuming that the MPLP problem is neither primitive nor dual degenerate, the set of all parameters with constraints of the same strength for the optimal solution constitutes a critical region $\boldsymbol{\Theta}$ [35].

In (8), for each parameter $\boldsymbol{\theta}$ and its corresponding optimal solution $\boldsymbol{x}^*(\boldsymbol{\theta})$, the constraints are divided into two parts: $\tilde{\boldsymbol{A}}\boldsymbol{x}^*(\boldsymbol{\theta}) = \tilde{\boldsymbol{b}} + \tilde{\boldsymbol{E}}\boldsymbol{\theta}$ contains strong constraints and $\overline{\boldsymbol{A}}\boldsymbol{x}^*(\boldsymbol{\theta}) < \overline{\boldsymbol{b}} + \overline{\boldsymbol{E}}\,\boldsymbol{\theta}$ contains weak constraints. $\boldsymbol{\theta}_1$ and $\boldsymbol{\theta}_2$ are in the same critical region $\boldsymbol{\Theta}$ only if $\tilde{\boldsymbol{A}}, \tilde{\boldsymbol{b}}, \tilde{\boldsymbol{E}}$ and $\overline{\boldsymbol{A}}, \overline{\boldsymbol{b}}, \overline{\boldsymbol{E}}$ are equal.

For example, consider a given parameter $\boldsymbol{\theta}_0$ and the corresponding optimal solution $\boldsymbol{x}^*(\boldsymbol{\theta}_0)$.

Let $\tilde{\boldsymbol{A}}_0\boldsymbol{x}^*(\boldsymbol{\theta}_0) = \tilde{\boldsymbol{b}}_0 + \tilde{\boldsymbol{E}}_0\boldsymbol{\theta}_0$ be the strong constraint and $\bar{\boldsymbol{A}}_0\boldsymbol{x}^*(\boldsymbol{\theta}_0) < \bar{\boldsymbol{b}}_0 + \bar{\boldsymbol{E}}_0\boldsymbol{\theta}_0$ be the weak constraint. The formula of the critical region $\boldsymbol{\Theta}_0$ containing the given parameter $\boldsymbol{\theta}_0$ is as follows

$$\Theta_0 = \left\{ \boldsymbol{\theta}_0 \mid \left(\bar{\boldsymbol{A}}_0\tilde{\boldsymbol{A}}_0{}^{-1}\tilde{\boldsymbol{E}}_0 - \bar{\boldsymbol{E}}_0 \right)\boldsymbol{\theta}_0 < \bar{\boldsymbol{b}}_0 - \bar{\boldsymbol{A}}_0\tilde{\boldsymbol{A}}_0{}^{-1}\tilde{\boldsymbol{b}}_0 \right\} \tag{9}$$

For any $\boldsymbol{\theta} \in \boldsymbol{\Theta}_0$, the optimal solution can be obtained directly from the mapping relation of Formula (10)

$$\boldsymbol{x}^*(\boldsymbol{\theta}) = \tilde{\boldsymbol{A}}_0{}^{-1}(\tilde{\boldsymbol{b}}_0 + \tilde{\boldsymbol{E}}_0\boldsymbol{\theta}) \tag{10}$$

3.2. OPF Model Reconstruction Based on Modified MPLP

The DC OPF model is a linear programming problem and is expressed as

$$\begin{aligned} \min \boldsymbol{z} = \boldsymbol{c}^{\boldsymbol{T}} \cdot \boldsymbol{D}_d & \\ s.t. \quad & 1^{\boldsymbol{T}} \cdot \boldsymbol{P} = 0 \\ & \boldsymbol{F} = \boldsymbol{G} \cdot \boldsymbol{P} \\ & \boldsymbol{P} = \boldsymbol{C} \cdot \boldsymbol{P}_g - (\boldsymbol{D} - \boldsymbol{D}_d) \\ & 0 \leq \boldsymbol{P}_g \leq \boldsymbol{P}_{gmax} \\ & \boldsymbol{F}_{min} \leq \boldsymbol{F} \leq \boldsymbol{F}_{max} \\ & 0 \leq \boldsymbol{D}_d \leq \boldsymbol{D} \end{aligned} \tag{11}$$

The objective function of the model is to minimize the system cutting load. The decision variable is the bus cutting load $\boldsymbol{D}_d$, and $\boldsymbol{c}$ is a constant vector whose elements represent the weight of each bus. The constraint conditions include the power balance constraint, transmission line capacity constraint, and nodal load constraint. $\boldsymbol{P}$ represents the net active power injected into the bus, the elements of $\boldsymbol{F}$ represent the active power of each branch, and $\boldsymbol{G}$ is the substitution distribution factor matrix, which reflects the relationship between the net injected active power of the buses and the active power of the branches. $\boldsymbol{C}$ is the generator-bus connection matrix: if generator k is connected to bus i, then $\boldsymbol{C}(k,i) = 1$; otherwise, $\boldsymbol{C}(k,i) = 0$. The elements of $\boldsymbol{D}$ represent the load demand of each bus. $\boldsymbol{P}_g$ is the output power of the generator, and $\boldsymbol{P}_{gmax}$ is the rated power of the generator. $\boldsymbol{F}_{min}$ and $\boldsymbol{F}_{max}$ represent the upper and lower limits of the active power flow on each transmission line.

The DC OPF model is transformed into the MPLP model according to the objective function and constraint conditions. For the objective function, the decision variables are $\boldsymbol{D}_d$ and $\boldsymbol{P}$. To satisfy the assumption that the MPLP problem is neither primitive nor dual degenerate, vectors $\boldsymbol{c}_1$ and $\boldsymbol{c}_2$ are added to the objective function, and the ith components of the two vectors are defined as $\boldsymbol{c}_1(i) = n + i$ and $\boldsymbol{c}_2(i) = i$, where n is a number much larger than i. The modified DC OPF model can be regarded as an MPLP problem, as shown in Formula (12)

$$\begin{aligned} \min \boldsymbol{z} = \boldsymbol{c}_1{}^{\boldsymbol{T}} \cdot \boldsymbol{D}_d + \boldsymbol{c}_2{}^{\boldsymbol{T}} \cdot \boldsymbol{P} & \\ s.t. \quad & 1^{\boldsymbol{T}} \cdot \boldsymbol{P} = 0 \\ & \boldsymbol{F}_{min} \leq \boldsymbol{G} \cdot \boldsymbol{P} \leq \boldsymbol{F}_{max} \\ & 0 \leq \boldsymbol{D}_d \leq \boldsymbol{D} \\ & \boldsymbol{P} - \boldsymbol{D}_d \leq \boldsymbol{C} \cdot \boldsymbol{P}_{gmax} - \boldsymbol{D} \end{aligned} \tag{12}$$

To consider generator failure and load variation, the generator state vector $\boldsymbol{S}_g$ and load vector $\boldsymbol{D}$ are selected to construct the parameter vector $\boldsymbol{\theta}$ of the MPLP problem. Compared with the standard MPLP form (8), the DC OPF model (12) is expressed as

$$\begin{aligned}
&\min \begin{bmatrix} \boldsymbol{c}_1^T & \boldsymbol{c}_2^T \end{bmatrix} \begin{bmatrix} \boldsymbol{D}_d \\ \boldsymbol{P} \end{bmatrix} \\
&s.t. \\
&\qquad \begin{bmatrix} \mathbf{0} & \mathbf{1}^{\mathrm{T}} \end{bmatrix} \begin{bmatrix} \boldsymbol{D}_d \\ \boldsymbol{P} \end{bmatrix} = [\mathbf{0}] + [\mathbf{0}]\boldsymbol{\theta} \\
&\qquad \begin{bmatrix} \mathbf{0} & \boldsymbol{G} \\ \mathbf{0} & -\boldsymbol{G} \\ -\mathbf{I} & \mathbf{I} \\ \mathbf{I} & \mathbf{0} \\ -\mathbf{I} & \mathbf{0} \end{bmatrix} \begin{bmatrix} \boldsymbol{D}_d \\ \boldsymbol{P} \end{bmatrix} \le \begin{bmatrix} \boldsymbol{F}_{max} \\ -\boldsymbol{F}_{min} \\ \mathbf{0} \\ \mathbf{0} \\ \mathbf{0} \end{bmatrix} + \begin{bmatrix} \mathbf{0} & \mathbf{0} \\ \mathbf{0} & \mathbf{0} \\ \boldsymbol{M} & -\mathbf{I} \\ \mathbf{0} & \mathbf{I} \\ \mathbf{0} & \mathbf{0} \end{bmatrix} \boldsymbol{\theta} \\
&\qquad \boldsymbol{\theta} = \begin{bmatrix} \boldsymbol{S}_g \\ \boldsymbol{D} \end{bmatrix} \\
&\qquad \boldsymbol{M} = \boldsymbol{C} \cdot diag(\boldsymbol{P}_{gmax})
\end{aligned} \tag{13}$$

In the matrix form of the DC optimal power flow model proposed in this paper, the decision variable $\boldsymbol{x}$ consists of $\boldsymbol{D}_d$ and $\boldsymbol{P}$. M represents the distribution of generators' output on buses. In the same transmission line status, the matrix $\boldsymbol{G}$ is a constant coefficient matrix, which meets the requirements of the standard formulation of the MPLP problem. This is also the theoretical core of the combination of the modified DC OPF model and the critical transmission line status proposed in this paper. When the parameter $\boldsymbol{\theta}$ changes due to a change in the generator fault state or load state, the optimal solution x may be adjusted accordingly. According to the critical region of the MPLP problem, if $\boldsymbol{\theta}$ is within a known critical region Θ, the optimal solution $\boldsymbol{x}^*(\boldsymbol{\theta})$ can be calculated using the mapping in Formula (10) instead of solving the general DC optimal power flow problem, which can save considerable calculation time.

To quickly generate critical regions with the MPLP method, this paper proposes a dynamic search method for critical regions. The specific steps are as follows:

First, a collection $\boldsymbol{\Phi}$ is introduced, and this collection includes the entire critical region of space containing parameter $\boldsymbol{\theta}$; initially, the set $\boldsymbol{\Phi}$ is empty. An initial sampling parameter $\boldsymbol{\theta}_0$ is introduced, and (7) is used to solve the general DC optimal power flow problem; then, according to Formula (9), the critical region $\boldsymbol{\Theta}_0$ can be calculated, including $\boldsymbol{\theta}_0$, and $\boldsymbol{\Theta}_0$ is added to the collection $\boldsymbol{\Phi}$.

Then, for each parameter $\boldsymbol{\theta}_i$ sampled, the set $\boldsymbol{\Phi}$ is traversed, and Formula (9) is used to determine whether the parameter belongs to the known critical region in the parameter space. If the parameter $\boldsymbol{\theta}_i$ belongs to the known critical region $\boldsymbol{\Theta}_k$, the optimal solution $\boldsymbol{x}*(\boldsymbol{\theta}_i)$ corresponding to the parameter can be calculated directly by using the mapping relation of Formula (10). If it does not belong to any known critical region, the general DC optimal power flow is determined, and a new critical region $\boldsymbol{\Theta}_i$ containing $\boldsymbol{\theta}_i$ is generated and added to the set $\boldsymbol{\Phi}$. Following this logic, all parameters $\boldsymbol{\theta}$ are searched, and the critical regions contained in the parameter space are generated.

4. Efficient Reliability Assessment Method

In this paper, the loss of load probability (LOLP) and expected energy not supplied (EENS) are chosen to describe the system reliability level. LOLP represents the average annual power shortage probability; EENS is the average number of kilowatt-hours of electricity lost per year. The calculation formulas are as follows

$$LOLP = \sum_{S \in \Omega_d} Prob_S \tag{14}$$

where Ω_d is the set of system fault states with load loss, that is $sum(\boldsymbol{D}_{dS}) > 0$. $Prob_S$ is the probability of system fault state S.

$$EENS = 8760 * \sum_{s \in \Omega_d} Prob_S \cdot sum(\boldsymbol{D}_{dS}) \tag{15}$$

where $sum(\boldsymbol{D}_{dS})$ is the total load loss of system fault state S.

The proposed method reduces the number of system states by using the randomness characteristic of the transmission line and generates critical transmission line status based on the transmission line status importance index. The complexity of system state analysis is reduced using the modified MPLP method. The proposed method first generates the set of critical transmission lines states offline before reliability assessment and then performs an online reliability assessment to meet the time requirement of short-term real-time assessment of power system reliability. The reliability assessment process is shown in Figure 2.

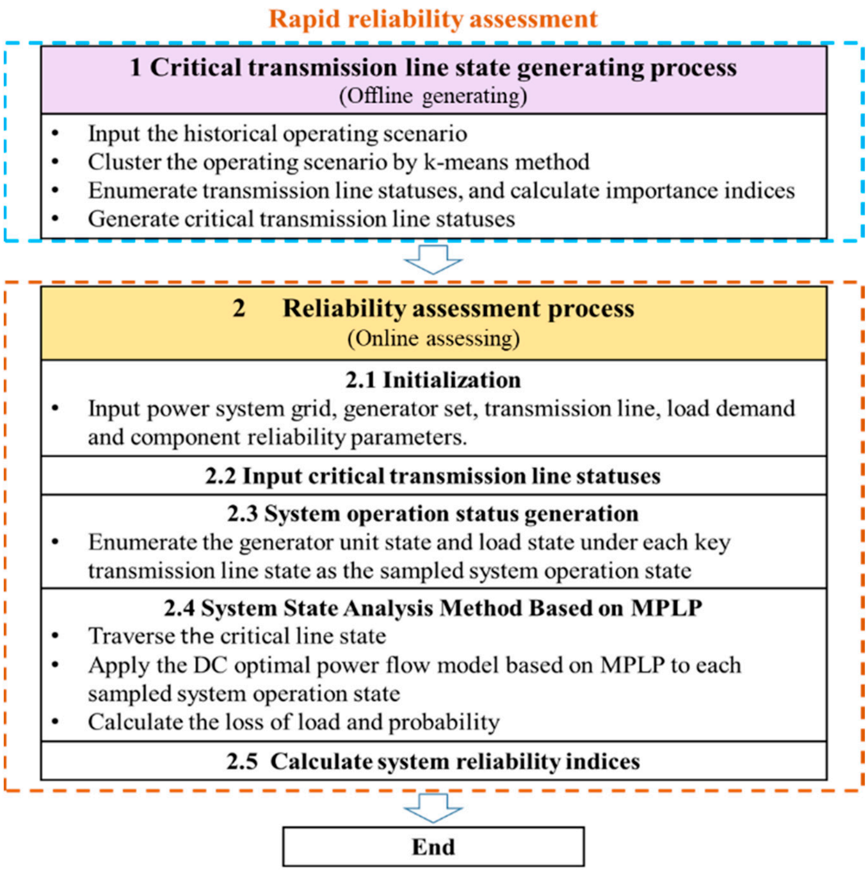

Figure 2. Flow chart of rapid reliability assessment.

5. Case Study

In this section, the RBTS system, the IEEE-RTS 79 system, the IEEE-RTS 96 system, and a practical provincial power system in China are used to test the performance of the proposed method. All experiments are carried out on a desktop computer equipped with a 3.10 GHz Intel Core i5-10500C CPU and 16 GB RAM. The proposed method is compared with the traditional enumeration method, nonsequential Monte Carlo method, and conventional MPLP method. System parameters are given based on the actual system operation set. In particular, the impacts of different types of faults that might happen in the transmission lines are considered in the actual system operation data set. The settings are as follows:

(1) Proposed method: in the system state generation process, the critical transmission line status is generated based on the importance index. The generator unit status is enumerated to third-order fault statuses and the load status is the peak load. In the state analysis process, the improved MPLP model is used for state analysis to calculate reliability indices. Then, the complete system reliability assessment is completed.

(2) Enumeration method: in the system state generation process, both the generator status and transmission line status are enumerated to third-order fault statuses. Consider a fixed peak load. Let the load reduction model adopt the ordinary DC optimal power flow model.

(3) Nonsequential Monte Carlo method: nonsequential Monte Carlo sampling is used to generate the system state. The load is a fixed peak load. The ordinary DC optimal power flow model is employed for load shedding calculation. The variance coefficient of LOLP is used as the assessment standard of calculation accuracy. Set the confidence level as $\alpha = 0.95$ and the convergence condition of the assessment results as $\beta \leq 1\%$.

(4) General MPLP method: in the state generation, the system state is generated by nonsequential Monte Carlo sampling. The load is a fixed peak load. In the state analysis, judge whether the sampled state meets the requirements of the MPLP problem. If it does, use the mapping relationship in the MPLP problem to solve it. If it does not, calculate the general DC optimal power flow model. The variance coefficient of LOLP is used as the assessment standard of calculation accuracy. Set the confidence level as to $\alpha = 0.95$. Let the convergence condition of the assessment results be $\beta \leq 1\%$.

5.1. Case I: RBTS

The RBTS adopted in this paper consists of 6 buses, 9 transmission lines, and 11 generators with a total installed capacity of 240 MW and a peak load of 185 MW. The system parameters are shown in [36]. The single-line diagram of RBTS is shown in Figure 3.

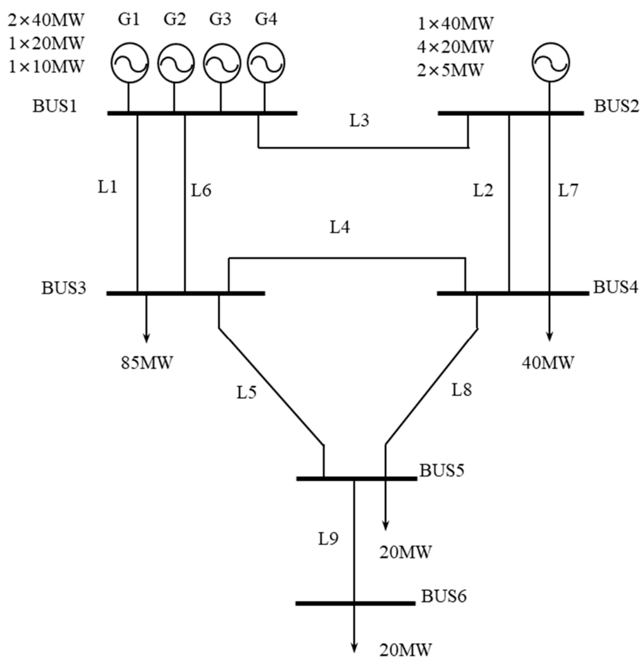

Figure 3. The single-line diagram of RBTS.

The efficiency of reliability assessment based on the enumeration method, the nonsequential Monte Carlo method, the conventional MPLP method, and the proposed method is shown in Table 1.

Table 1. Reliability assessment results of the RBTS.

Methods	Sample Number	LOLP	EENS (MWh/a)	Calculation Time (s)
Enumeration	30,160	0.0104	1167.8	125.02
Nonsequential Monte Carlo	1,011,999	0.0098	1056.0	4194.82
Conventional MPLP	913,414	0.0107	1254.3	3578.45
Proposed method	5336	0.0103	1164.2	11.47

It can be seen from Table 1 that the error of the proposed method is less than 1% compared with the reliability assessment results of the enumeration method. However, the proposed method only needs 11.47 s to accomplish the reliability evaluation, which is 9% of the time required by the enumeration method, 0.2% of the time required by the nonsequential Monte Carlo method, and 0.3% of the general conventional method. Therefore, the proposed method can significantly improve the efficiency of reliability assessment.

As seen from Table 1, the method proposed in this paper considers only 5336 system states, while the enumeration method needs to consider 30,160 system states. Based on the critical transmission line status generating method, the sampled number of system states is reduced by 82.3%, the reliability assessment efficiency is improved by 10.8 times, and the accuracy error is less than 1%. However, the nonsequential Monte Carlo method requires 1,011,999 systems because it has a poor convergence effect in the RBTS system, resulting in a large number of samples, a long calculation time, and low assessment accuracy. The conventional MPLP method, in contrast to the non-sequential Monte Carlo method, has slightly improved the speed of state analysis and evaluation efficiency. Nevertheless, the conventional MPLP method has weak convergence ability when the number of system states increases.

5.2. Case II: IEEE-RTS 79 System

The IEEE-RTS 79 system adopted in this paper consists of 24 buses, 38 transmission lines, and 32 generators, with a total installed capacity of 3405 MW and a peak load of 2850 MW. The system parameters are shown in [37]. The single-line diagram of IEEE-RTS 79 system is shown in Figure 4.

The comparison results are shown in Table 2.

It is clear from Table 2 that the absolute error of the system loss of load probability is 0.0001. The relative error is as low as 0.1%. The absolute error of the system power shortage expectation is 971 MWh/a. The relative error is 0.7%. The proposed method can ensure a reliability assessment error within 1%. In addition, the proposed method converges in 25.81 s, which is 1.09% of the time required by the enumeration method and 3.9% of the time required by the nonsequential Monte Carlo method and 4.2% of the conventional MPLP method. Therefore, the proposed method can significantly improve the reliability assessment efficiency by at least 23 times. In contrast with the enumeration method, the nonsequential Monte Carlo method, and the conventional MPLP method, the number of system states required for analysis is respectively reduced by 97.4%, 90.3%, and 91.8%. This is mainly due to the reduction that the proposed method affects in the number of system states and the complexity of system state analysis. Although the conventional MPLP method also reduces the number of system states and the time for system analysis, due to the strong randomness of sampling system states. Fewer system states can meet the requirements of the MPLP problem and the mapping relationship cannot be fully used to avoid the optimal power flow calculation.

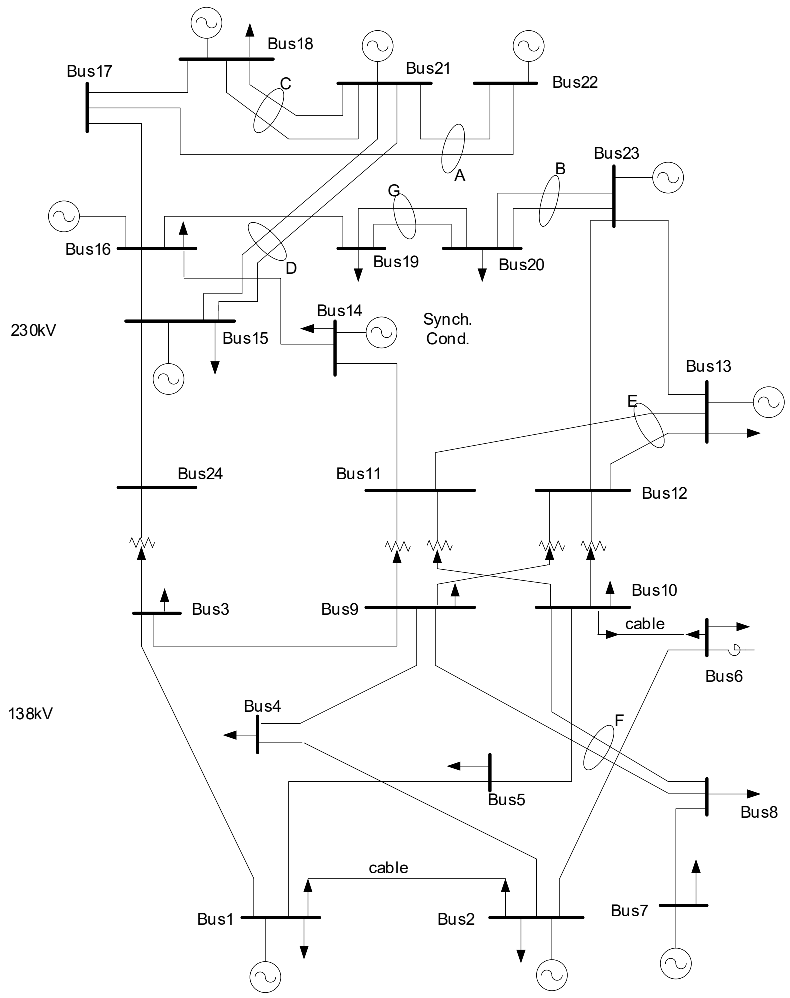

Figure 4. The single-line diagram of IEEE-RTS 79 system.

Table 2. Reliability assessment results of the IEEE-RTS 79 system.

Methods	Sample Number	LOLP	EENS (MWh/a)	Calculation Time/(s)
Enumeration	392,518	0.0853	129,561	2355.11
Nonsequential Monte Carlo	108,222	0.0846	127,549	649.33
Conventional MPLP	127,612	0.0937	148,921	607.49
Proposed method	10,580	0.0852	128,590	25.81

5.3. Case III: IEEE-RTS 96 System

The IEEE-RTS 96 system adopted in this paper consists of 73 buses, 120 transmission lines, and 99 generators with a total installed capacity of 10,215 MW and a peak load of 8550 MW. The system parameters are shown in [38].

The comparison results are shown in Table 3.

Table 3. Reliability assessment results of the IEEE-RTS 96 system.

Methods	Sample Number	LOLP	EENS (MWh/a)	Calculation Time(h)
Enumeration	35,949,211	0.0144	24,876	9374.42
Nonsequential Monte Carlo	709,173	0.0139	24,704	145.33
Conventional MPLP	849,610	0.0160	27,521	123.68
Proposed method	99,020	0.0142	24,848	3.67

According to the results in Table 3, the proposed method reduces the sampled number of system states by 99.7% and the assessment accuracy error is less than 1% than the enumeration method. Compared with the nonsequential Monte Carlo method, the efficiency of the reliability assessment is improved by 39.6 times. The efficiency of the reliability assessment is improved by 33.7 times in contrast to the conventional MPLP method. It can be found that as the system scale increases, the proposed method will more significantly improve the assessment efficiency. This is because an increasing number of system states can be analyzed by using the mapping relationship in the modified MPLP method as the system scale increases, which avoids time-consuming OPF calculations.

5.4. Case IV: Scalability Test

A provincial power grid in China adopted in this paper consists of 1393 buses, 2033 transmission lines, and 220 generators with a total installed capacity of 64,702.61 MW and a peak load of 39,009.29 MW. The generator states and transmission line states are enumerated as first-order fault states.

The result is shown in Table 4.

Table 4. Reliability assessment results of a provincial power grid in China.

Methods	Sample Number	LOLP	EENS (MWh/a)	Calculation Time/(h)
Enumeration	449,514	0.0017	93.73	26.85
Nonsequential Monte Carlo	93,928	0.0016	92.97	5.67
Conventional MPLP	101,756	0.0018	94.02	4.99
Proposed method	4420	0.0017	93.33	0.14

According to the results in Table 4, the proposed method can be successfully used in the actual power system, which has good accuracy and high efficiency compared with the others.

6. Conclusions

This paper proposes a modified MPLP method for improving the efficiency of power system reliability assessment. On the one hand, this method reduces the number of samples by generating critical system states based on the importance index of the transmission lines. On the other hand, to reduce the complexity of system state analysis, the optimal power flow model is modified to the multiparameter linear programming method, and the optimal solution can be calculated by linear operations under certain conditions. Case studies show that compared with the conventional methods, the proposed method can improve reliability assessment efficiency by 10–40 times without losing accuracy. Furthermore, with the increase in the system size, the improvement in efficiency increases. This fully verifies the effectiveness and superiority of the proposed method.

Author Contributions: Conceptualization, J.Z.; investigation, J.Z. and S.P.; methodology, J.Z., S.P. and Y.Y.; funding acquisition, Y.Y. and Z.L.; project administration, Z.Z. and H.Y.; validation, J.Z.;

writing—original draft, J.Z.; writing—review and editing, S.P. and Y.L. All authors have read and agreed to the published version of the manuscript.

Funding: This work was supported by the Power Planning Project of Guangdong Power Grid Corporation (031000QQ00210009).

Data Availability Statement: The data set can be found by contacting the corresponding author.

Acknowledgments: This research was supported by the Power Planning Project of Guangdong Power Grid Corporation (031000QQ00210009). All authors are very grateful for their support for the research.

Conflicts of Interest: The authors declare no conflict of interest.

Nomenclature

OPF	Optimal power flow
MPLP	Multiparameter linear programming
RBTS	Roy Billinton test system
LOLP	Loss of load probability
EENS	Expected energy not supplied
I_{tra}	Traditional importance index of transmission lines
I_{pro}	Fault probability importance index of transmission lines
F_i	Actual active power flow of line i
$F_i{}^{max}$	Upper limit of the active power capacity of line i
w_i	Weighting factor of line i
N_l	Number of transmission lines in the system
N_d	Number of fault transmission lines in the system
m	Integer index of I_{tra}
P_c	Probability of failure of the Nd transmission line
U_i	Forced outage rate of the transmission lines with failures
U_j	Forced outage rate of the transmission lines without failures
M_{ij}	Initial clustering center
N_L	Number of clusters
D_{ki}	Euclidean distance from the kth point to the i^{th} cluster center
G_{kj}	Value of the k^{th} point on curve j
N_c	Number of curves
N_i	Number of points in the i^{th} cluster
L_{ki}	Value of the kth point in the i^{th} cluster on curve j
P_l	Probability of the l^{th} operating scenario
N_c	Number of points clustered in the l^{th} operating scenario
N	Total number of points on the curve
R	Comprehensive importance index of the system state
I_l	Importance index of operation scenario l
N_S	Number of system operation scenarios selected after clustering
$\boldsymbol{z}$	Objective function
$\boldsymbol{x}$	Decision variable
$\boldsymbol{c}$	Constant coefficient
$\boldsymbol{\theta}$	Parameter vector
$\boldsymbol{\Theta}$	Critical region
$\boldsymbol{\Phi}$	Critical region set
$\boldsymbol{D}_d$	Bus cutting load
$\boldsymbol{P}$	Net active power injected into the bus
$\boldsymbol{F}$	Active power of each branch
$\boldsymbol{G}$	Substitution distribution factor matrix
$\boldsymbol{C}$	Generator-bus connection matrix
$\boldsymbol{D}$	Load demand of each bus
$\boldsymbol{P}_g$	Output power of the generators

P_{gmax} Rated power of the generators
F_{min} Lower limits of the active power flow on each transmission line
F_{max} Upper limits of the active power flow on each transmission line
S_g Generator state vector

References

1. Lin, C.; Hu, B. Event-triggered load frequency control based on age-of-information. *IEEE Trans. Power Syst.* **2022**, 1–13. [CrossRef]
2. Širá, E.; Kotulič, R.; Kravčáková Vozárová, I.; Daňová, M. Sustainable development in EU countries in the framework of the europe 2020 strategy. *Processes* **2021**, *9*, 443. [CrossRef]
3. Yang, L.; Huang, W.; Guo, C.; Zhang, D.; Xiang, C.; Yang, L.; Wang, Q. Multi-objective optimal scheduling for multi-renewable energy power system considering flexibility constraints. *Processes* **2022**, *10*, 1401. [CrossRef]
4. Zhironkin, S.; Rybár, R. Sustainable development processes for renewable energy technology. *Processes* **2022**, *10*, 1363. [CrossRef]
5. Naik, J.; Bisoi, R.; Dash, P. Prediction interval forecasting of wind speed and wind power using modes decomposition based low rank multi-kernel ridge regression. *Renew. Energy* **2018**, *129*, 357–383. [CrossRef]
6. Ericsson, G.N. Information security for electric power utilities (EPUs)—CIGRE developments on frameworks, risk assessment, and technology. *IEEE Trans. Power Delivery* **2009**, *24*, 1174–1181. [CrossRef]
7. Aghaei, J.; Barani, M.; Shafie-Khah, M.; De La Nieta, A.A.S.; Catalão, J.P. Risk-constrained offering strategy for aggregated hybrid power plant including wind power producer and demand response provider. *IEEE Trans. Sustain. Energy* **2015**, *7*, 513–525. [CrossRef]
8. Prajapati, V.K.; Mahajan, V. Reliability assessment and congestion management of power system with energy storage system and uncertain renewable resources. *Energy* **2021**, *215*, 119134. [CrossRef]
9. Liu, H.; Sun, Y.; Wang, P.; Cheng, L.; Goel, L. A novel state selection technique for power system reliability evaluation. *Electr. Power Syst. Res.* **2008**, *78*, 1019–1027. [CrossRef]
10. Jia, Y.; Wang, P.; Han, X.; Tian, J.; Singh, C. A fast contingency screening technique for generation system reliability evaluation. *IEEE Trans. Power Syst.* **2013**, *28*, 4127–4133. [CrossRef]
11. Thompson, D.R.; Green, R.O.; Keymeulen, D.; Lundeen, S.K.; Mouradi, Y.; Nunes, D.C.; Castaño, R.; Chien, S.A. Rapid spectral cloud screening onboard aircraft and spacecraft. *IEEE Trans. Geosci. Remote Sens.* **2014**, *52*, 6779–6792. [CrossRef]
12. Dai, H.; Zhang, H.; Wang, W. A support vector density-based importance sampling for reliability assessment. *Reliab. Eng. Syst. Saf.* **2012**, *106*, 86–93. [CrossRef]
13. Guo, Y.; Chen, Z.; Zhang, X.; Pan, E. Reliability modeling and maintenance optimization of manufacturing system based on stochastic flow network and markov process. *J. Shanghai Jiaotong Univ.* **2021**, *55*, 229.
14. Schweitzer, E.O.; Whitehead, D.; Zweigle, G.; Ravikumar, K.G. Synchrophasor-based power system protection and control applications. In Proceedings of the 63rd Annual Conference for Protective Relay Engineers, College Station, TX, USA, 29 March–1 April 2010; pp. 1–10.
15. He, J.; Sun, Y.; Kirschen, D.; Singh, C.; Cheng, L. State-space partitioning method for composite power system reliability assessment. *IET Gener. Transm. Distrib.* **2010**, *4*, 780–792. [CrossRef]
16. Huang, W.; Du, E.; Capuder, T.; Zhang, X.; Zhang, N.; Strbac, G.; Kang, C. Reliability and vulnerability assessment of multi-energy systems: An energy hub based method. *IEEE Trans. Power Syst.* **2021**, *36*, 3948–3959. [CrossRef]
17. Wang, Y.; Guo, C.; Wu, Q. A cross-entropy-based three-stage sequential importance sampling for composite power system short-term reliability evaluation. *IEEE Trans. Power Syst.* **2013**, *28*, 4254–4263. [CrossRef]
18. Da Silva, A.M.L.; González-Fernández, R.A.; Flávio, S.A.; Manso, L.A. Composite reliability evaluation with renewable sources based on quasi-sequential monte carlo and cross entropy methods. In Proceedings of the 2014 International Conference on Probabilistic Methods Applied to Power Systems (PMAPS), Durham, UK, 7–10 July 2014; pp. 1–6.
19. Bao, M.; Ding, Y.; Singh, C.; Shao, C. A multi-state model for reliability assessment of integrated gas and power systems utilizing universal generating function techniques. *IEEE Trans. Smart Grid.* **2019**, *10*, 6271–6283. [CrossRef]
20. Song, G.; Chen, H.; Guo, B. A layered fault tree model for reliability evaluation of smart grids. *Energies* **2014**, *7*, 4835–4857. [CrossRef]
21. Shu, Z.; Jirutitijaroen, P.; da Silva, A.M.L.; Singh, C. Accelerated state evaluation and latin hypercube sequential sampling for composite system reliability assessment. *IEEE Trans. Power Syst.* **2014**, *29*, 1692–1700. [CrossRef]
22. Anghel, M.; Werley, K.A.; Motter, A.E. Stochastic model for power grid dynamics. In Proceedings of the 2007 40th Annual Hawaii International Conference on System Sciences (HICSS'07), Big Island, HI, USA, 3–6 January 2007; p. 113.
23. Lin, C.; Hu, B.; Shao, C.; Li, W.; Li, C.; Xie, K. Delay-dependent optimal load frequency control for sampling systems with demand response. *IEEE Trans. Power Syst.* **2022**, *37*, 4310–4324. [CrossRef]
24. Xu, Q.; Yang, Y.; Liu, Y.; Wang, X. An improved latin hypercube sampling method to enhance numerical stability considering the correlation of input variables. *IEEE Access* **2017**, *5*, 15197–15205. [CrossRef]
25. Xu, C.; Yonggang, G.; Wenpeng, Z.; Cheng, T. Diagnosis method on the mechanical failure of high voltage circuit breakers based on factor analysis and SVM. *Trans. China Electro Tech. Soc.* **2005**, *27*, 26–32.
26. Zhao, Y.; Kuang, J.; Xie, K.; Li, W.; Yu, J. Dimension reduction based non-parametric disaggregation for dependence modeling in composite system reliability evaluation. *IEEE Trans. Power Syst.* **2020**, *36*, 159–168. [CrossRef]

27. Urgun, D.; Singh, C. A hybrid Monte Carlo simulation and multi label classification method for composite system reliability evaluation. *IEEE Trans. Power Syst.* **2018**, *34*, 908–917. [CrossRef]
28. Lin, C.; Hu, B.; Shao, C.; Niu, T.; Cheng, Q.; Li, C.; Xie, K. An analysis of delay-constrained consensus-based optimal algorithms in virtual power plants. *ISA Trans.* **2015**, *125*, 189–197. [CrossRef]
29. Sildir, H.; Sarrafi, S.; Aydin, E. Uncertainty Propagation Based MINLP approach for artificial neural network structure reduction. *Processes* **2022**, *10*, 1716. [CrossRef]
30. Guo, J.; Han, M.; Zhan, G.; Liu, S. A Spatio-Temporal Deep Learning Network for the Short-Term Energy Consumption Prediction of Multiple Nodes in Manufacturing Systems. *Processes* **2022**, *10*, 476. [CrossRef]
31. Liu, Z.; Hou, K.; Jia, H.; Zhao, J.; Wang, D.; Mu, Y.; Zhu, L. A Lagrange multiplier based state enumeration reliability assessment for power systems with multiple types of loads and renewable generations. *IEEE Trans. Power Syst.* **2020**, *36*, 3260–3270. [CrossRef]
32. Lukashevich, A.; Maximov, Y. Power Grid Reliability Estimation via Adaptive Importance Sampling. *IEEE Control Syst. Lett.* **2021**, *6*, 1010–1015. [CrossRef]
33. Zhu, T. A New Methodology of Analytical Formula Deduction and Sensitivity Analysis of EENS in Bulk Power System Reliability Assessment. In Proceedings of the 2006 IEEE PES Power Systems Conference and Exposition, Atlanta, GA, USA, 29 October–1 November 2006; pp. 825–831.
34. Silva, P.R.D.; Aragão, M.E.; Trierweiler, J.O.; Trierweiler, L.F. MILP Formulation for Solving and Initializing MINLP Problems Applied to Retrofit and Synthesis of Hydrogen Networks. *Processes* **2022**, *8*, 1102. [CrossRef]
35. Ji, Y.; Thomas, R.J.; Tong, L. Probabilistic forecasting of real-time LMP and network congestion. *IEEE Trans. Power Syst.* **2016**, *32*, 831–841. [CrossRef]
36. Billinton, R.; Kumar, S.; Chowdhury, N.; Chu, K.; Debnath, K.; Goel, L.; Khan, E.; Kos, P.; Nourbakhsh, G.; Oteng-Adjei, J. A reliability test system for educational purposes-basic data. *IEEE Trans. Power Syst.* **1989**, *4*, 1238–1244. [CrossRef]
37. Subcommittee, P.M. IEEE reliability test system. *IEEE Trans. Power Appar. Syst.* **1979**, *PAS-98*, 2047–2054. [CrossRef]
38. Grigg, C.; Wong, P.; Albrecht, P.; Allan, R.; Bhavaraju, M.; Billinton, R.; Chen, Q.; Fong, C.; Haddad, S.; Kuruganty, S. The IEEE reliability test system-1996. A report prepared by the reliability test system task force of the application of probability methods subcommittee. *IEEE Trans. Power Syst.* **1999**, *14*, 1010–1020. [CrossRef]